Controlling swarms of robots with global inputs: breaking symmetry

Aaron T. Becker

N338 Engineering Building 1 (D), Houston, TX 77204-4005, USA

Abstract

Roboticists, biologists, and chemists are now producing large populations of simple robots, but controlling large populations of robots with limited capabilities is difficult, due to communication and onboard-computation constraints. This chapter provides controllability proofs for control of mobile robots that move in a 2D workspace where each robot receives exactly the same control inputs.

We focus on two types of control: when control inputs are the desired angular and linear velocity for the robots, and secondly when control inputs are the desired direction and speed for the robots. Both use broadcast control inputs: the first uses control inputs specified in the local reference frame of each robot, while the second uses control inputs specified in the global reference frame. Each method allows steering each robot to a desired goal location in $O(n^2)$ time, but the second option enables a class useful of swarm manipulation tasks to be accomplished efficiently.

Keywords: micro robot, nano robot, global inputs, nonprehensile, under actuation

2016 MSC: 00-01, 99-00

1. introduction

Micro and nano robotics hold great promise for precision material delivery and for micro construction. According to Sitti et al. "One of the highest potential scientific and societal impacts of small-scale (millimeter and submillimeter size) untethered mobile robots would be their healthcare and bioengineering applications" [1].

The flagship application for precision delivery is targeted therapy [2, 3, 4, 5, 6]. The current dominant practice in cancer treatment uses chemotherapy applied systemically, but has associated collateral damage to hair follicles and other fast-growing tissue. Successful precision delivery would steer toxins directly to tumors.

Health care is also a driver for micro construction, which includes minimally invasive surgery [7, 8, 9, 10], and tissue engineering [11, 12, 13, 14, 15]. The surgical industry is rapidly switching to minimally invasive surgery, which places surgical instruments at the end of long, slender kinematic chains and inserts this apparatus through small incisions, called ports, in the body. There is a desire to shrink the size and number of ports, but as the ports decrease in size, the kinematic chain to the external world becomes less rigid. This flexibility makes dexterity difficult and limits surgical forces.

Long before the advent of minimally invasive surgery, authors dreamed of doing away with incisions and kinematic chains by shrinking the surgeon and tools into a compact submarine-like vehicle that could be piloted through the many fluid-filled lumens of the body. This dream is in its infancy. There has been notable progress with pill cameras, tiny cameras that record a passage through the digestive track, from swallowing to expelling.

Shrinking the surgeon to make a capable autonomous robot is hard for two main limitations: power and computation. As the length of the axis ℓ decreases, the surface area decreases as ℓ^2, but the volume at ℓ^3. This relationship is plotted in Fig. 1. Nanocars are perhaps the smallest possible robots, but at 1.4×1.7 nm they are smaller than the smallest transistors currently in production (14 nm, beginning in 2014 by Intel). This limited volume effectively prevents onboard computation in nano robots and severely limits computation in microrobots. Power is limited for the same reason because stored power is also a function of volume.

In the 2014 Disney movie *Big Hero 6*, the protagonist Hiro offers a pro-

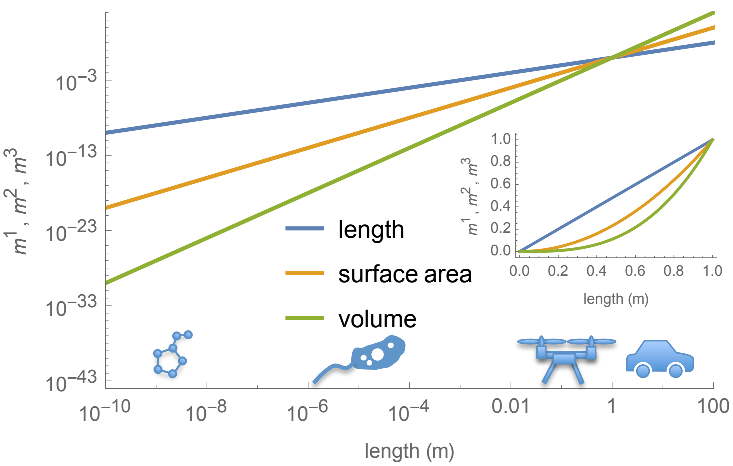

Figure 1: Scaling laws show that microrobots loose volume faster than surface area and much faster than length as length decreases. This is significant because onboard power and computation is proportional to volume, while forces required for propulsion are proportional to length and surface area.

found view into the future by manufacturing a swarm of 10^5 microbots. Hiro controls them to self-assemble, to build structures, and to transport goods and materials. While the "microrobots" of the film are fantasy, the ideas are rooted in reality. Today, micro- and nanorobots can be produced in extremely large quantities. Once a manufacturing process is developed, the marginal cost of producing one additional robot is small. Microrobots can be fabricated using microelectromechanical system (MEMS) techniques, e.g. scratch-drive micro robots [16, 17, 18, 19]. These robots are 60 by 250 microns in size, and can be mass-produced with many robots tiled on a single silicon wafer. Perhaps the best examples of large populations are robotic *nanocars*—synthetic molecules with integrated axles, rolling wheels, and light-driven molecular motors, that are 1.4×1.7 nm in size [20, 21, 22, 23, 24, 25, 26, 27, 28, 29, 30]. These are routinely produced in tremendous quantities—a batch the size of an aspirin tablet contained $\approx 4 \times 10^{19}$ nanocars [21]. This dwarfs the number of automobiles

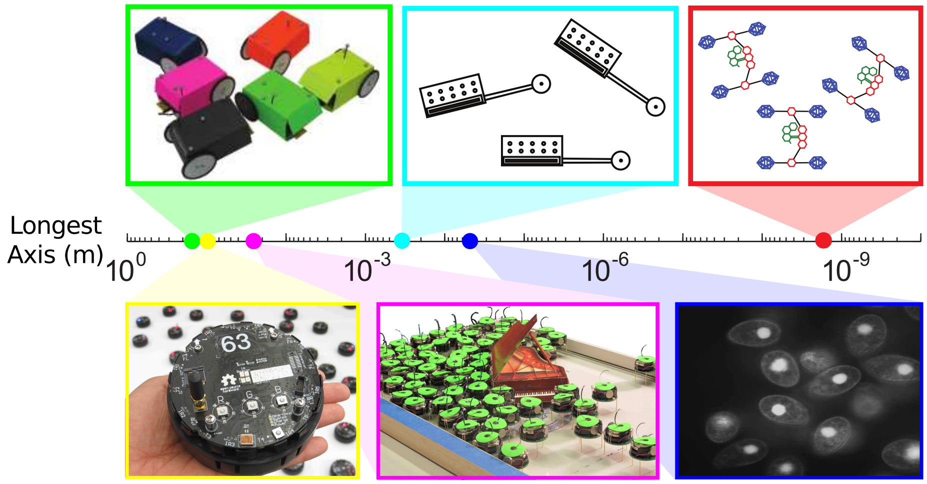

Figure 2: Uniform control inputs are ubiquitous in micro/nano robotics. Top: differential-drive robots with broadcast control [38], microrobots controlled by shared electrical signal [17], light-driven nanocars [21]. Bottom: r-one swarm under broadcast control [39], photophile kilobot robots [40], and magnetically steered protozoa [41].

produced in the history of the world—90 million automobiles were manufactured in 2014 [31]. Also, biological agents such as bacteria [32, 33, 34, 3, 35] and paramecium [36, 37] can be grown to achieve large swarms.

Ideally, we would design a system that would allow each robot to be controlled individually. However, next-generation micro- and nanorobotic systems have minimal on-board processing and communications bandwidth. The lack of significant on-board computation makes autonomous operation infeasible. Sending individual control signals to each robot requires communications bandwidth that scales with population sizes. Because these systems are only useful when their populations are immense, the bandwidth required for individual unit control is impractical.

Instead, this chapter focuses on systems with *uniform* control inputs. Some representative systems are shown in Fig. 2: light-driven nanocars are *uniformly* actuated by a certain wavelength of light, scratch-drive microrobots are *uniformly* actuated by varying the electric potential across a substrate, and multi-

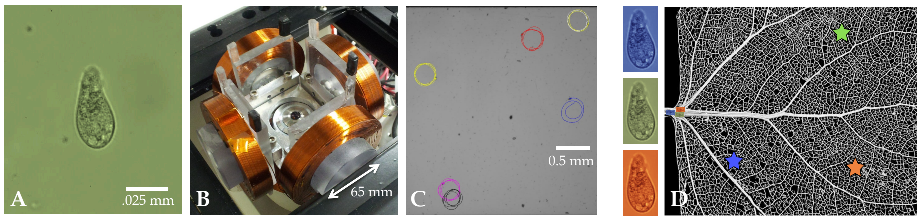

Figure 3: Example of uniform control inputs. (A) After feeding iron particles to ciliate eukaryon (*Tetrahymena pyriformis*) and magnetizing the particles with a permanent magnet, the cells can be turned by changing the orientation of an external magnetic field (B). Using two orthogonal Helmholz electromagnets, Kim et al. demonstrated steering many living magnetized T. pyriformis cells [41, 57]. All cells are steered by the same global field (C). (D) Target applications are in biological vascular networks, such as the vasculature in this cottonwood leaf. Photo: Royce Bair/Flickr/Getty Images.

robot systems are *uniformly* controlled by a broadcast radio signal. Other uniform input examples include the magnetic resonant microrobots of Hsi-Wen et al. [42]; the magnetic helical swimming micro- and nanorobots of Ghosh and Fischer [43], Tottori et al. [44], and Schlüre and Nelson et al. [45, 46]; the magnetic microparticles of Diller and Floyd et al. [47, 48, 49]; the magnetic milli-scale capsules of Vartholomeos et al. [50]; the magnetic particles studied by Snezhko et al. and Orduño et al. [51, 52, 53, 54]; and the tumbling magnetic microrobots of [55]. Biological examples include the electric-field controlled paramecium studied by Hashimoto et al. [36] and Hasegawa et al. [37], galvanotactic the electrokinetic and optically controlled bacteria demonstrated by Steager et al. [32], the magnetic-field controlled bacteria demonstrated by Martel et al. [33, 34, 3, 35] and magnetic-field steered protozoa demonstrated by Ou et al. [56]. Figure 3 shows an example of bacteria steered by a global control input provided by an external magnetic field.

2. Breaking symmetry

A swarm of robots controlled by a 2 DoF (degree of freedom) signal is inherently under-actuated since each robot has two to six DoF. To make robots behave differently requires a mechanism to break symmetry from the control input. Breaking symmetry enables the same control input to steer individual robots to different locations.

Our previous work applied ensemble control theory [58, 59, 60, 61, 62, 63, 64, 65, 66, 67, 68, 69] and control Lyapunov functions [70] to steer swarms of robots. Our work, [39, 41, 57, 71, 72, 73, 74, 75, 76, 77], applied these techniques to steer swarms of single-celled organisms using an external magnetic field [41], because they enabled swarms of robots to be asymptotically driven toward goal states—see overview in Fig. 3. On a larger scale, but using similar control laws, we applied ensemble control to drive a swarm of motors to desired velocities using the uniform magnetic gradient of a clinical MRI scanner [78]. All this work has one serious drawback: the complexity of the control law increases quadratically with the number of robots, as shown in Figs. 4 and 8. Because swarms of robots can now number in the millions, progress requires techniques that scale sublinearly (or are constant) with population size. Section 4 discusses techniques that use collisions with obstacles to break the symmetry of the control input. These techniques can often exploit the environment to efficiently reconfigure the swarm. A concluding medical example: our work using an MRI to self-assemble Gauss gun components floating inside a spinal-fluid model relied on obstacles to break symmetry and achieve quasi-independent control of three components [7].

3. Breaking Symmetry With Robot Inhomogeneity

Many micro robots, including all those in Fig. 2, have kinematics that match the *kinematic unicycle* model. This model describes each robot with an x, y location and heading θ, with two control inputs; linear velocity $v(t)$ and angular velocity $\omega(t)$. $v(t)$ and $\omega(t)$ are functions of time, but we assume that the same $v(t)$ and $\omega(t)$ are applied to every robot

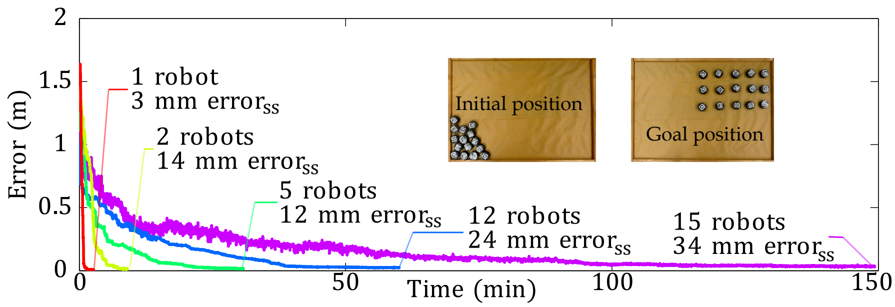

Figure 4: Current state-of-the-art using uniform control (robots receive *exactly the same* motion commands) when control inputs are specified in the local reference frame of each robot [77]. Robots can be steered to desired positions, but required time grows quadratically with number of robots.

With this model, consider a collection of n unicycles that each roll without slipping. Following the terminology of [58, 59, 64], we call this collection an *ensemble* and describe the configuration of the ith robot by $\mathbf{q}_i = [x_i, y_i, \theta_i]^\top$ and its configuration space by $\mathcal{Q} = \mathbb{R}^2 \times \mathbb{S}^1$. The global control inputs are the forward speed $u \in \mathbb{R}$ and turning rate $\omega \in \mathbb{R}$. We assume that each robot has a nonzero parameter v_i that scales the linear velocity and a unique nonzero parameter ϵ_i that scales the turning rate ($|\epsilon_i| \neq |\epsilon_j| \ \forall\ i, j$). These v_i, ϵ_i values may arise from stochastic processes during manufacturing [16], or as design decisions [80]. The kinematics of the unicycle are given by

$$\dot{\mathbf{q}}_i(t) = v_i u(t) \begin{bmatrix} \cos\theta_i \\ \sin\theta_i \\ 0 \end{bmatrix} + \epsilon_i \omega(t) \begin{bmatrix} 0 \\ 0 \\ 1 \end{bmatrix}. \tag{1}$$

If v_i is zero the robot cannot move. Similarly, $\epsilon_i = 0$ prevents the robot from turning. On a collection of differential-drive robots, these parameters can be mapped to unique wheel sizes and $\epsilon_i = v_i$.

We model our robotic system with a discrete-time model. We can simplify (1) by splitting each ΔT time step into two stages with piecewise constant inputs. During the first stage of round k we command the robots to turn in place ϕ, and during the second stage command the linear movement $u(k)$.

$$k = \left\lfloor \frac{t}{\Delta T} \right\rfloor$$

$$\Big[u(t), \omega(t)\Big] = \begin{cases} \big[0, \quad \frac{2}{\Delta T}\phi\big] & t - k\Delta T < \frac{\Delta T}{2} \\ \big[\frac{2}{\Delta T}u(k), 0\big] & \text{else} \end{cases} \tag{2}$$

A control law that steers each robot to their goal alternates between having all robots turn in place and then commanding all the robots to move forwards or backwards. During the first stage of round k we command the robots to turn in place ϕ, and during the second stage command the linear movement

$$u(k) = -\frac{1}{n}\sum_{i=1}^{n}\left(x_i(k)\cos(\theta_i(k)) + y_i(k)\sin(\theta_i(k))\right) \tag{3}$$

This controller requires that either all robots turn at slightly different rates or that robots when commanded to turn have stochastic variations. Either condition is possible by naturally occurring [57] or designed parameter variations during robot construction [16]. As long as ϕ meets the constraints on the sampling frequency given by the Nyquist frequency, our globally asymptotically stable control results follow. The control policy (3) is easy to implement, never increases the summed distance of the ensemble from the goal, and is robust to standard models of noise.

Figure 5 shows simulations of the first 100 commands to an ensemble of two robots. Below each drawing of the robots at a specified number of turns is a plot of the sum squared distance of each robot to their goal locations. This error function is always quadratic. At each step, the linear velocity control input is chosen that minimizes the error function. This results in a control law that is globally asymptotically stable. Fig. 6 shows the same procedure with six robots. The error function is always quadratic. The fact that the error function is quadratic for arbitrary goal locations and any number of robots was surprising to us, so we made an interactive online demonstration you can use to steer robots to goal locations [81]. Alternately, purchase multiple RC cars that all have the same control frequency and practice steering them to goals. This experiment costs less than $20, and is popular with all ages.

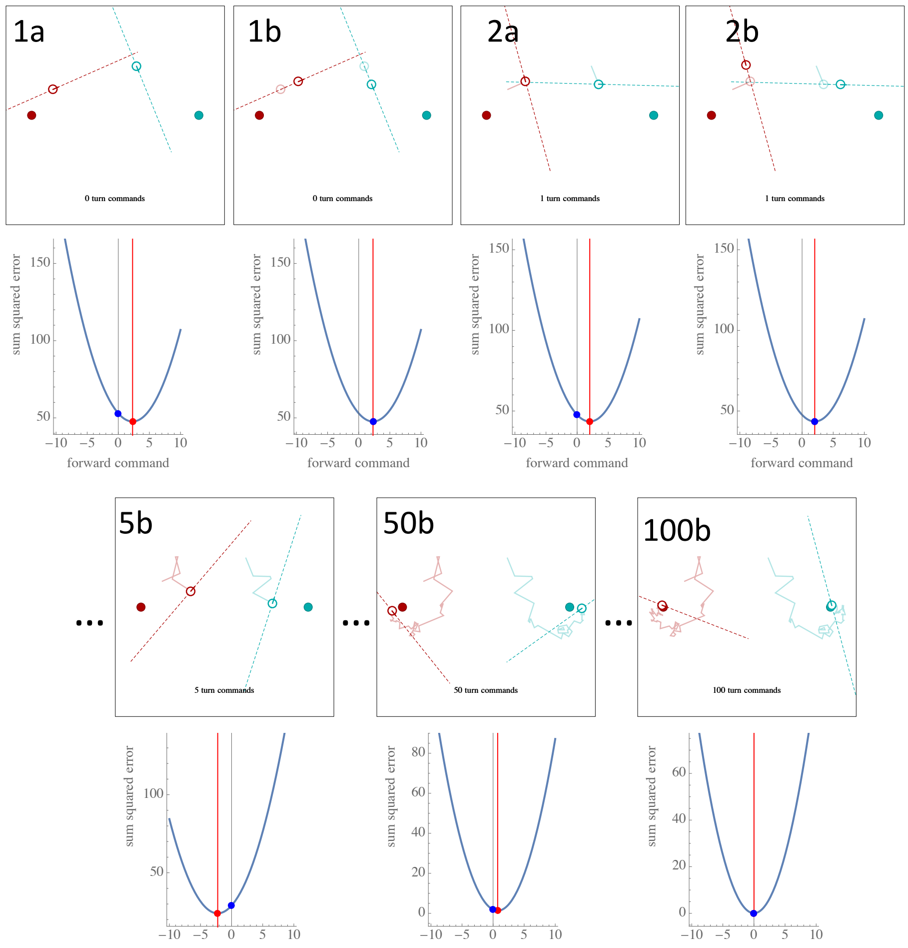

Figure 5: Ensemble control consists of (a) commanding each robot to rotate in place, and then (b) commanding each robot to move a distance d that is selected to minimize the average distance of the swarm to their respective goals. The top row shows the robots, drawn as a circle with a tick mark indicating the forward direction of the robot and the dashed lines achievable positions by moving forward or backward. The bottom row shows the average distance of the swarm to their respective goals as a function of the forward command applied to all the robots. This function is always quadratic for any number of robots. After the turn in step 1a, a commanded distance of $+2.1$ minimizes the average distance error. In step 2 a forward command of $+2.0$ minimizes the error. By step 100 the robots are each on their respective goal locations. Simulation is available online at [81].

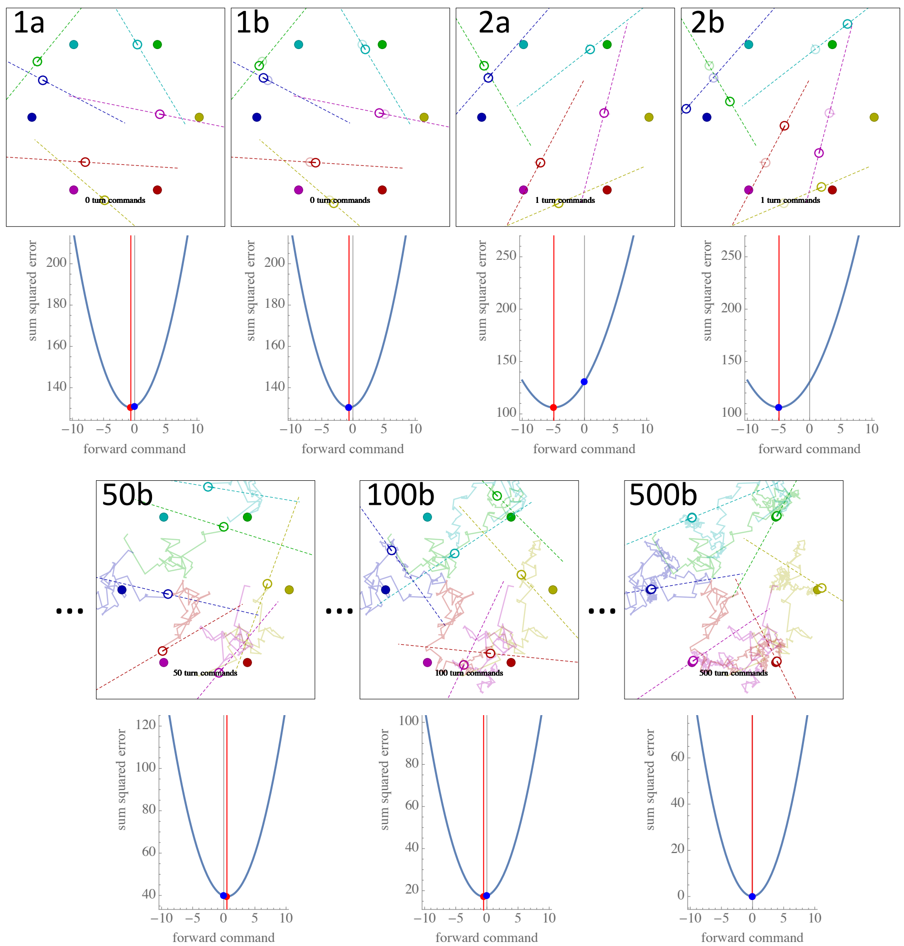

Figure 6: Ensemble control with six robots. The average distance of the swarm to their respective goals as a function of the forward command applied to all the robots is always quadratic for any number of robots. Convergence with six robots requires more time than with two robots. Simulation is available online at [81].

4. Breaking Symmetry with Obstacles

Global inputs dictate that every robot receives the same control commands. The previous section exploited the fact that all robots, especially at the micro scale, experience stochastic disturbances and so react differently to inputs. This section instead exploits the fact that robots often move in an environment rich with obstacles. These obstacles exert position-dependent forces on the robots, and can therefore often be used to efficiently manipulate the swarm towards a desired configuration.

Model: At micro-scales, viscous forces dominate inertial forces [79], giving a simple kinematic model

$$c_i \dot{x}_i = u_x, \quad c_i \dot{y}_i = u_y.$$

Here the control input $[u_x, u_y]$ is globally applied to robots with positions $[x_i, y_i]$ for $i \in [1, n]$.

4.1. Nonprehensile manipulation

In *nonprehensile manipulation*, a robot affects its environment without grasping [82, 83, 84]. In some ways, our problem formulation is the inverse of nonprehensile manipulation. Rather than just use a robot to restructure the environment, we use the environment to restructure a population of robots.

We can also use a large population of robots for traditional nonprehensile tasks, such as transporting objects using the flow of the robots [85], and manipulating an object too heavy for a single robot. Our control formulation enables efficient control of this kind of transport.

4.2. BlockWorld *Abstraction*

We illustrate our points with a simplified BlockWorld abstraction. The workspace is a rectangular $m_1 \times m_2$ grid in which each square is marked either *free*, *fixed*, or *robot*. All *robots* are controlled by a shared input command from the set $\{\uparrow, \rightarrow, \leftarrow, \downarrow, \emptyset\}$, and can move horizontally and vertically in the grid, as

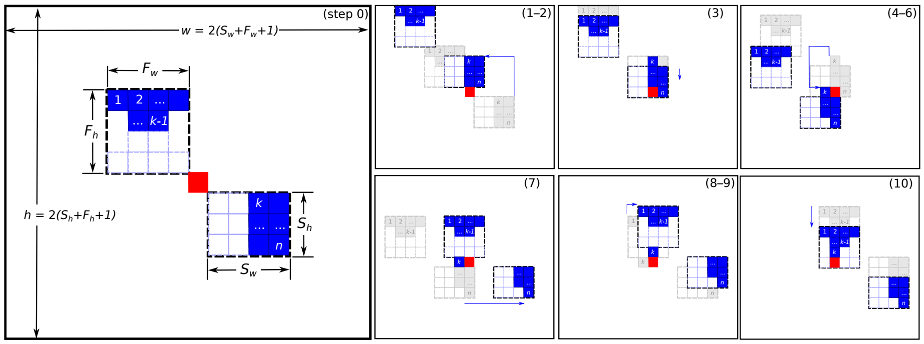

Figure 7: A single rectangular obstacle is sufficient to enable position control of n robots. We provide an $O(n^2)$ algorithm to accomplish this. Shown above are frames from moving the kth robot into position. The robots are initially within the box at $S(t)$, which is of width S_w and height S_h. We want to move these robots to their final positions within a box at $F(t)$, which is of width F_w and height F_h and disjoint from $S(t)$. Given a simple square obstacle O, the algorithm requires at least $S_w + F_w + 1$ space on the left, $S_w + F_w$ on the right, $S_h + F_h + 1$ above, and $S_h + F_h$ below the obstacle.

long as there are no *fixed* squares stopping the robot. The boundary of the grid is composed of *fixed* squares.

The general case of motion-planning in a world composed of even a single robot and both *fixed* and *moveable* squares is in the complexity class PSPACE-complete [86]. Adding an additional robot does not decrease this complexity: given any single-robot problem, we can place a second robot in the boundary of the world and surround it with *fixed* squares without changing the original problem's complexity. Still, there are many tractable subproblems.

4.3. Position control

This section presents an algorithm to control the position of n robots using a single obstacle. We employ the BlockWorld abstraction, where the robots and the obstacle are unit squares. Each call to Algorithm 1 moves one robot from its starting position to its goal position.

Notation. The starting position of the kth robot in world coordinates is $k^W(0)$, its desired final position is k^W_{goal}, and its position at time t is $k^W(t)$. We define fixed-size, axis-aligned bounding boxes S and F such that $k^W(0) \in S^W(0)$ and $k^W_{\text{goal}} \in F^W(0)\ \forall k \in [1, n]$. The bottom left corners of S and F are $[S^W_x(t), S^W_y(t)]$ and $[F^W_x(t), F^W_y(t)]$, and are of width S_w, F_w and height S_h, F_h. Because all robots are identical, without loss of generality the robot indices are arranged in raster-scan order left-to-right, top-to-bottom in S and top-to-bottom, left-to-right in F. We note that the position of the kth robot may be specified in local reference frame: $k^W(t) = F^W(t) + k^F(t)$. The unmoving obstacle is located at $[O^W_x, O^W_y]$. We assume the obstacle position $O_{x,y}$, the starting positions $S_{x,y}$, and the final positions $F_{x,y}$ are disjoint. Without loss of generality, we will assume that S is to the lower right of the obstacle and F is to the upper left of the obstacle, as illustrated in Fig. 7.

Procedure. At the beginning of the kth call, the time is t, the bounding boxes S and F have been returned to their initial positions on opposite corners of O, the first $k-1$ robots have been moved to their proper positions in F, the remaining robots are in their original columns in S, and O is between S and F. The kth robot starts in position $[k^W_x(t), k^W_y(t)]$ and should be moved to $[k^W_{\text{goal},x}, k^W_{\text{goal},y}]$.

The algorithm consists in "popping" the kth robot out of the $S(t)$ bounding box (steps 1–3), pushing the kth robot to the correct x coordinate relative to $F_x(t)$ (steps 4–7), pushing the kth robot to the correct y coordinate relative to $F_y(t)$ (steps 8–10), and returning the S and F bounding boxes to their original positions on either side of O (steps 11–12).

The commanded distance to move the kth robot from $k^W(0)$ to the final destination k^W_{goal} is bounded by:

$$\text{Commanded distance}(k) \leq 2(2S_h + S_w + F_h + F_w + 2)$$

The total distance commanded for position control of n robots is the sum:

$$\begin{aligned}\text{Commanded distance} &= \sum_{k=1}^{n} \text{Commanded distance}(k) \\ &\leq 2n(2S_h + S_w + F_h + F_w + 2).\end{aligned}$$

Algorithm 1 $\textsc{PositionControl}(S, F, O, k)$

move $\uparrow$ until $S_y^W(t) > O_y^W$
move $\leftarrow$ until $k_x^W(t) = O_x^W$
move $\downarrow$ until $k_y^W(t) > S_y^W(t) + S_h$
move $\uparrow$ until $S_y^W(t) > O_y^W$
move $\leftarrow$ until $S_x^W(t) < O_y^W - S_w$
move $\downarrow$ until $k_y^W(t) = O_y^W$
move $\rightarrow$ until $k_x^W(t) = F_{\text{goal},x} + k_{\text{goal},x}^F$
move $\uparrow$ 1
move $\rightarrow$ 1
move $\downarrow$ until $k_y^W(t) = F_{\text{goal},y}^W + k_{\text{goal},y}^F$
move $\uparrow$ until $F_y^W(t) > O_y^W$
move $\leftarrow$ until $F_x^W(t) < O_x^W - F_w$

Analysis. Algorithm 1 always requires $12n$ control switches. The worst-case running time for Algorithm 1 occurs when S and F are sparse and/or have large aspect ratios, and the algorithm runs in $O(n \cdot \max\{S_w, S_h, F_w, F_h\})$ time. For more reasonable arrays, when S and F are dense with aspect ratios near 1, the running time approaches $O(n\sqrt{n})$.

Algorithm 1 requires at least $S_w + F_w + 1$ free space to the left, $S_w + F_w$ to the right, $S_h + F_h + 1$ above, and $S_h + F_h$ below the obstacle:

$$(2S_h + 2F_h + 1) \times (2S_w + 2F_w + 1)\,.$$

Simulation. Simulation results are shown in Fig. 8 for five arrangements with an increasing number of robots. We compare the total distance moved and commanded with the *LAP distance*—the shortest distance according to the Linear Assignment Problem using Manhattan distance. Because all robots are interchangeable, the LAP distance reduces to

$$\text{LAP} = \sum_{k=1}^{n} \left| k_x^W(0) - k_{\text{goal},x}^W \right| + \left| k_y^W(0) - k_{\text{goal},y}^W \right| .$$

5. Conclusion

Manufacturing micro robots has a host of challenges, but there is significant progress by roboticists, biologists, and chemists, who are now producing large populations of simple robots [32, 34, 21]. Controlling large populations of robots with limited capabilities is difficult, due to communication and onboard-computation constraints. Rather than focus on a particular design, this chapter reviewed recent work on controlling large numbers of agents using a global input. Section 3 examined global controls given in the local reference frame of each robot, in the form of angular and velocity commands. Section 4 examined a class of controllers that applies controls in a global references frame.

For an in depth analysis of the complexity of motion planning problem with global inputs see [89, 90, 91, 92, 93]. For recent work on swarm manipulation and shape control of a swarm see Shiva and Becker[94, 95, 96].

References

[1] M. Sitti, H. Ceylan, W. Hu, J. Giltinan, M. Turan, S. Yim, E. Diller, Biomedical applications of untethered mobile milli/microrobots, Proceedings of the IEEE 103 (2) (2015) 205–224. doi:10.1109/JPROC.2014.2385105.

[2] F. Munoz, G. Alici, W. Li, A review of drug delivery systems for capsule endoscopy, Advanced drug delivery reviews 71 (2014) 77–85.

[3] S. Martel, Bacterial microsystems and microrobots, Biomedical Microdevices 14 (6) (2012) 1033–1045. doi:10.1007/s10544-012-9696-x. URL http://dx.doi.org/10.1007/s10544-012-9696-x

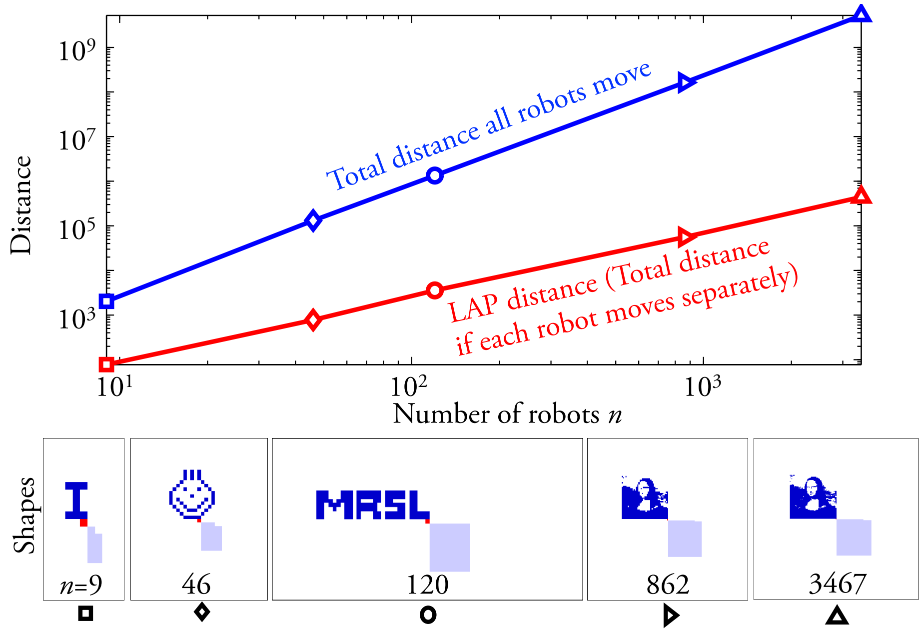

Figure 8: The required number of moves using our algorithm [40], which employs a single square obstacle to rearrange n square-shaped robots, that all respond identically to a global signal. The log-log plot compares *Total distance*—the sum of the moves made by every robot, with *LAP distance*—the shortest distance according to the Linear Assignment Problem using Manhattan distance. In each metric moving $\{\uparrow, \rightarrow, \leftarrow, \downarrow\}$ one unit counts as one move. These were calculated for five patterns. Dark blue is target position, red is obstacle, light blue is initial configuration. The outline shows the minimum required free space. See hardware implementation and simulation at [87] and code at [88]. This chapter reviews techniques that do not grow polynomially with population size.

[4] S. Martel, Microrobotics in the vascular network: present status and next challenges, Journal of Micro-Bio Robotics 8 (1) (2013) 41–52.

[5] S. Fusco, G. Chatzipirpiridis, K. M. Sivaraman, O. Ergeneman, B. J. Nelson, S. Pané, Chitosan electrodeposition for microrobotic drug delivery, Advanced healthcare materials 2 (7) (2013) 1037–1044.

[6] R. W. Carlsen, M. R. Edwards, J. Zhuang, C. Pacoret, M. Sitti, Magnetic steering control of multi-cellular bio-hybrid microswimmers, Lab on a Chip 14 (19) (2014) 3850–3859.

[7] A. T. Becker, O. Felfoul, P. E. Dupont, Toward tissue penetration by MRI-powered millirobots using a self-assembled Gauss gun, in: IEEE International Conference on Robotics and Automation (ICRA), Seattle, WA, USA, 2015.

[8] S. Yim, E. Gultepe, D. H. Gracias, M. Sitti, Biopsy using a magnetic capsule endoscope carrying, releasing, and retrieving untethered microgrippers, Biomedical Engineering, IEEE Transactions on 61 (2) (2014) 513–521.

[9] C. Yu, J. Kim, H. Choi, J. Choi, S. Jeong, K. Cha, J.-o. Park, S. Park, Novel electromagnetic actuation system for three-dimensional locomotion and drilling of intravascular microrobot, Sensors and Actuators A: Physical 161 (1) (2010) 297–304.

[10] P. Miloro, E. Sinibaldi, A. Menciassi, P. Dario, Removing vascular obstructions: a challenge, yet an opportunity for interventional microdevices, Biomedical microdevices 14 (3) (2012) 511–532.

[11] I. J. Fox, G. Q. Daley, S. A. Goldman, J. Huard, T. J. Kamp, M. Trucco, Use of differentiated pluripotent stem cells as replacement therapy for treating disease, Science 345 (6199) (2014) 1247391.

[12] S. Tasoglu, C. Yu, H. Gungordu, S. Guven, T. Vural, U. Demirci, Guided and magnetic self-assembly of tunable magnetoceptive gels, Nature communications 5.

[13] S. Tasoglu, E. Diller, S. Guven, M. Sitti, U. Demirci, Untethered micro-robotic coding of three-dimensional material composition, Nature communications 5.

[14] E. Diller, M. Sitti, Three-dimensional programmable assembly by untethered magnetic robotic micro-grippers, Advanced Functional Materials 24 (28) (2014) 4397–4404.

[15] J. Giltinan, E. Diller, C. Mayda, M. Sitti, Three-dimensional robotic manipulation and transport of micro-scale objects by a magnetically driven capillary micro-gripper, in: Robotics and Automation (ICRA), 2014 IEEE International Conference on, IEEE, 2014, pp. 2077–2082.

[16] B. Donald, C. Levey, C. McGray, I. Paprotny, D. Rus, An untethered, electrostatic, globally controllable MEMS micro-robot, J. of MEMS 15 (1) (2006) 1–15.

[17] B. Donald, C. Levey, I. Paprotny, Planar microassembly by parallel actuation of MEMS microrobots, J. of MEMS 17 (4) (2008) 789–808.

[18] B. R. Donald, C. G. Levey, I. Paprotny, D. Rus, Planning and control for microassembly of structures composed of stress-engineered MEMS microrobots, The International Journal of Robotics Research 32 (2) (2013) 218–246.
URL `http://ijr.sagepub.com/content/32/2/218.abstract`

[19] I. Paprotny, C. Levey, B. Donald, Turning-rate selective control: A new method for independent control of stress-engineered MEMS microrobots, in: Robotics: Science and Systems (RSS), Vol. VIII, Sydney, Australia, 2012.

[20] Y. Shirai, A. J. Osgood, Y. Zhao, K. F. Kelly, J. M. Tour, Directional control in thermally driven single-molecule nanocars, Nano Letters 5 (11) (2005) 2330–2334. `doi:10.1021/nl051915k`.

[21] P.-T. Chiang, J. Mielke, J. Godoy, J. M. Guerrero, L. B. Alemany, C. J. Villagómez, A. Saywell, L. Grill, J. M. Tour, Toward a light-driven motorized nanocar: Synthesis and initial imaging of single molecules, ACS Nano 6 (1) (2011) 592–597. doi:10.1021/nn203969b.

[22] G. Vives, J. Kang, K. F. Kelly, J. M. Tour, Molecular machinery: Synthesis of a "nanodragster", Organic Letters 11 (24) (2009) 5602–5605. doi:10.1021/ol902312m.
URL http://dx.doi.org/10.1021/ol902312m

[23] G. Vives, J. M. Tour, Synthesis of single-molecule nanocars, Acc. Chem. Res 42 (2009) 473–487.

[24] G. Vives, J. M. Tour, Synthesis of a nanocar with organometallic wheels, Tetrahedron Lett. 50 (2009) 1427–1430.

[25] T. Sasaki, G. Guerrero, A. D. Leonard, J. M. Tour, Nanotrains and self-assembled two-dimensional arrays built from carboranes linked by hydrogen bonding of dipyridones, Nano Res. 1 (2008) 412–419.

[26] T. Sasaki, J. M. Guerrero, J. M. Tour, The assembly line: Self-assembling nanocars, Tetrahedron 64 (2008) 8522–8529.

[27] T. Sasaki, J. M. Tour, Synthesis of a new photoactive nanovehicle: Nanoworm, Org. Lett. 10 (2008) 897–900.

[28] J.-F. Morin, T. Sasaki, Y. Shirai, J. M. Guerrero, J. M. Tour, Synthetic routes toward carborane-wheeled nanocars, J. Org. Chem. 72 (2007) 9481–9490.

[29] Y. Shirai, J.-F. Morin, T. Sasaki, J. Guerrero, J. M. Tour, Recent progress on nanovehicles, Chem. Soc. Rev. 35 (2006) 1043–1055.

[30] Y. Shirai, A. J. Osgood, Y. Zhao, Y. Yao, L. Saudan, H. Yang, C. Yu-Hung, L. B. Alemany, T. Sasaki, J.-F. Morin, J. Guerrero, K. F. Kelly, J. M. Tour, Surface-rolling molecules, J. Am. Chem. Soc. 128 (2006) 4854–4864.

[31] OICA, Production statistics, http://www.oica.net/category/production-statistics/ (Jul. 2015).

[32] E. B. Steager, M. Sakar, D. H. Kim, V. Kumar, G. J. Pappas, Electrokinetic and optical control of bacterial microrobots., J. of Micromechanics and Microengineering 21 (3).

[33] O. Felfoul, M. Mohammadi, L. Gaboury, S. Martel, Tumor targeting by computer controlled guidance of magnetotactic bacteria acting like autonomous microrobots, in: Intelligent Robots and Systems (IROS), 2011 IEEE/RSJ International Conference on, 2011, pp. 1304–1308. doi:10.1109/IROS.2011.6094991.

[34] D. de Lanauze, O. Felfoul, J.-P. Turcot, M. Mohammadi, S. Martel, Three-dimensional remote aggregation and steering of magnetotactic bacteria microrobots for drug delivery applications, The International Journal of Robotics Research.
URL http://ijr.sagepub.com/content/early/2013/11/11/0278364913500543

[35] S. Martel, S. Taherkhani, M. Tabrizian, M. Mohammadi, D. de Lanauze, O. Felfoul, Computer 3D controlled bacterial transports and aggregations of microbial adhered nano-components, Journal of Micro-Bio Robotics 9 (1-2) (2014) 23–28.

[36] K. Hashimoto, K. Takahashi, N. Ogawa, H. Oku, Visual feedback control for a cluster of microorganisms, in: International Joint Conference SICE-ICASE, 2006, pp. 4198–4201.

[37] T. Hasegawa, N. Ogawa, H. Oku, M. Ishikawa, A new framework for microrobotic control of motile cells based on high-speed tracking and focusing, in: IEEE Int. Conf. Rob. Aut., 2008, pp. 3964–3969.

[38] A. Becker, C. Onyuksel, T. Bretl, Feedback control of many differential-drive robots with uniform control inputs, in: IEEE/RSJ International Con-

ference on Intelligent Robots and Systems (IROS), Vilamoura, Portugal, 2012, pp. 2256–2262.

[39] A. Becker, J. McLurkin, Exact range and bearing control of many differential-drive robots with uniform control inputs, in: IEEE/RSJ International Conference on Intelligent Robots and Systems (IROS), Tokyo, Japan, 2013, pp. 3338–3343.

[40] A. Becker, G. Habibi, J. Werfel, M. Rubenstein, J. McLurkin, Massive uniform manipulation: Controlling large populations of simple robots with a common input signal, in: IEEE/RSJ International Conference on Intelligent Robots and Systems (IROS), Tokyo, Japan, 2013, pp. 520–527.

[41] A. Becker, Y. Ou, P. Kim, M. Kim, A. Julius, Feedback control of many magnetized tetrahymena pyriformis cells by exploiting phase inhomogeneity, in: IEEE/RSJ International Conference on Intelligent Robots and Systems (IROS), Tokyo, Japan, 2013, pp. 3317–3323.

[42] H.-W. Tung, D. R. Frutiger, S. Panè, B. J. Nelson, Polymer-based wireless resonant magnetic microrobots, in: IEEE International Conference on Robotics and Automation, 2012, pp. 715–720.

[43] A. Ghosh, P. Fischer, Controlled propulsion of artificial magnetic nanostructured propellers, Nano Letters 9 (6) (2009) 2243–2245. `doi:10.1021/nl900186w`.
URL `http://dx.doi.org/10.1021/nl900186w`

[44] S. Tottori, L. Zhang, F. Qiu, K. Krawczyk, A. Franco-Obregón, B. J. Nelson, Magnetic helical micromachines: Fabrication, controlled swimming, and cargo transport, Advanced Materials 24 (811).

[45] S. Schürle, K. E. Peyer, B. E. Kratochvil, B. J. Nelson, Holonomic 5-DOF magnetic control of 1D nanostructures, in: IEEE Int. Conf. Rob. Aut., 2012, pp. 1081–1086.

[46] F. Qiu, B. J. Nelson, Magnetic helical micro-and nanorobots: Toward their biomedical applications, Engineering 1 (1) (2015) 21–26.

[47] S. Floyd, E. Diller, C. Pawashe, M. Sitti, Control methodologies for a heterogeneous group of untethered magnetic micro-robots, Int. J. Robot. Res. 30 (13) (2011) 1553–1565.

[48] E. Diller, S. Floyd, C. Pawashe, M. Sitti, Control of multiple heterogeneous magnetic microrobots in two dimensions on nonspecialized surfaces 28 (1) (2012) 172–182.

[49] E. Diller, J. Giltinan, M. Sitti, Independent control of multiple magnetic microrobots in three dimensions, The International Journal of Robotics Research 32 (5) (2013) 614–631.
URL `http://ijr.sagepub.com/content/32/5/614.abstract`

[50] P. Vartholomeos, M. Akhavan-Sharif, P. E. Dupont, Motion planning for multiple millimeter-scale magnetic capsules in a fluid environment, in: IEEE Int. Conf. Rob. Aut., 2012, pp. 1927–1932.

[51] M. Belkin, A. Snezhko, I. S. Aranson, W.-K. Kwok, Driven magnetic particles on a fluid surface: pattern assisted surface flows., Phys Rev Lett 99 (15) (2007) 158301.
URL `http://www.biomedsearch.com/nih/Driven-magnetic-particles-fluid-surface/17995219.html`

[52] A. Snezhko, I. S. Aranson, W.-K. Kwok, Surface wave assisted self-assembly of multidomain magnetic structures., Phys Rev Lett 96 (7) (2006) 078701.
URL `http://www.biomedsearch.com/nih/Surface-wave-assisted-self-assembly/16606148.html`

[53] A. Snezhko, M. Belkin, I. S. Aranson, W.-K. Kwok, Self-assembled magnetic surface swimmers., Phys Rev Lett 102 (11) (2009) 118103.

URL http://www.biomedsearch.com/nih/Self-assembled-magnetic-surface-swimmers/19392241.html

[54] C. Orduño, A. Becker, T. Bretl, Motion primitives for path following with a self-assembled robotic swimmer, in: IEEE Int. Rob. and Sys., Vilamoura, Portugal, 2012, pp. 1440–1446.

[55] W. Jing, N. Pagano, D. Cappelleri, A tumbling magnetic microrobot with flexible operating modes, in: Robotics and Automation (ICRA), 2013 IEEE International Conference on, 2013, pp. 5514–5519. doi:10.1109/ICRA.2013.6631368.

[56] Y. Ou, D. H. Kim, P. Kim, M. J. Kim, A. A. Julius, Motion control of magnetized tetrahymena pyriformis cells by magnetic field with model predictive control, Int. J. Rob. Res. 32 (1) (2013) 129–139.

[57] P. S. S. Kim, A. Becker, Y. Ou, A. A. Julius, M. J. Kim, Imparting magnetic dipole heterogeneity to internalized iron oxide nanoparticles for microorganism swarm control, Journal of Nanoparticle Research 17 (3) (2015) 1–15.

[58] R. W. Brockett, N. Khaneja, On the control of quantum ensembles, in: T. Djaferis, I. Schick (Eds.), System Theory: Modeling, Analysis and Control, Kluwer Academic Publishers, 1999.

[59] N. Khaneja, Geometric control in classical and quantum systems, Ph.D. thesis, Harvard University (2000).

[60] J.-S. Li, N. Khaneja, Ensemble controllability of the Bloch equations, in: IEEE Conf. Dec. Cont., San Diego, CA, 2006, pp. 2483–2487.

[61] J.-S. Li, N. Khaneja, Control of inhomogeneous quantum ensembles, Physical Review A (Atomic, Molecular, and Optical Physics) 73 (3) (2006) 030302. doi:10.1103/PhysRevA.73.030302.

[62] J.-S. Li, Control of inhomogeneous ensembles, Ph.D. thesis, Harvard University (May 2006).

[63] J.-S. Li, N. Khaneja, Ensemble control of linear systems, in: IEEE Conf. Dec. Cont., New Orleans, LA, USA, 2007, pp. 3768–3773. doi:10.1109/CDC.2007.4434971.

[64] J.-S. Li, N. Khaneja, Ensemble control of Bloch equations, IEEE Trans. Automat. Contr. 54 (3) (2009) 528–536. doi:10.1109/TAC.2009.2012983.

[65] S. Li, A new perspective on control of uncertain complex systems, in: IEEE Conf. Dec. Cont., 2009, pp. 708–713.

[66] J.-S. Li, Ensemble control of finite-dimensional time-varying linear systems, IEEE Trans. Automat. Contr. 56 (2) (2011) 345–357.

[67] J. Ruths, Optimal control of inhomogeneous ensembles, Ph.D. thesis, Washington University in St. Louis, St. Louis, Missouri, United States (June 2011).

[68] J. Ruths, J.-S. Li, A multidimensional pseudospectral method for optimal control of quantum ensembles, The Journal of Chemical Physics 134 (4) (2011) 044128–8.

[69] K. Das, D. Ghose, Broadcast control mechanism for positional consensus in multiagent systems, Control Systems Technology, IEEE Transactions on PP (99) (2015) 1–1. doi:10.1109/TCST.2015.2388732.

[70] Z. Artstein, Stabilization with relaxed controls, Nonlinear Analysis 15 (11) (1983) 1163–1170.

[71] A. Becker, T. Bretl, Motion planning under bounded uncertainty using ensemble control, in: Robotics: Science and Systems (RSS), Zaragoza, Spain, 2010.
URL http://www.roboticsproceedings.org/rss06/p38.pdf

[72] A. Becker, T. Bretl, Approximate steering of a unicycle under bounded model perturbation using ensemble control 28 (3) (2012) 580–591.

[73] A. Becker, T. Bretl, Approximate steering of a plate-ball system under bounded model perturbation using ensemble control, in: IEEE/RSJ International Conference on Intelligent Robots and Systems (IROS), Vilamoura, Portugal, 2012, pp. 5353–5359.

[74] A. Becker, Ensemble control of robotic systems, Ph.D. thesis, University of Illinois at Urbana-Champaign, http://hdl.handle.net/2142/34221 (Aug. 2012).

[75] A. Becker, "Range and Bearing Control of an Ensemble of Robots": http://www.mathworks.com/matlabcentral/fileexchange/38190 (Sep. 2012).
URL http://www.mathworks.com/matlabcentral/fileexchange/38190

[76] P. S. Soo Kim, A. Becker, Y. Ou, A. A. Julius, M. J. Kim, Swarm control of cell-based microrobots using a single global magnetic field, in: Ubiquitous Robots and Ambient Intelligence (URAI), 2013 10th International Conference on, IEEE, Jeju, Korea, 2013, pp. 21–26.

[77] A. Becker, C. Onyuksel, T. Bretl, J. McLurkin, Control of many differential-drive robots with uniform control inputs, Int. J. Rob. Res. 33 (2014) 1626–1644. doi:10.1177/0278364914543481.

[78] A. Becker, O. Felfoul, P. E. Dupont, Simultaneously powering and controlling many actuators with a clinical MRI scanner, in: Intelligent Robots and Systems (IROS 2014), 2014 IEEE/RSJ International Conference on, IEEE, 2014, pp. 2017–2023.

[79] E. M. Purcell, Life at low reynolds number, American Journal of Physics 45 (1) (1977) 3–11. doi:10.1119/1.10903.
URL http://dx.doi.org/10.1119/1.10903

[80] K. E. Peyer, L. Zhang, B. J. Nelson, Bio-inspired magnetic swimming microrobots for biomedical applications, Nanoscale.

[81] A. T. Becker, http://demonstrations.wolfram.com/search.html?query=aaron-becker, Mathematica Demonstrations (2010).
URL http://demonstrations.wolfram.com/search.html?query=aaron-becker

[82] K. Lynch, Locally controllable manipulation by stable pushing, IEEE Trans. Robot. Automat. 15 (2) (1999) 318–327.

[83] O. C. Goemans, K. Goldberg, A. F. van der Stappen, Blades: a new class of geometric primitives for feeding 3d parts on vibratory tracks, in: Int. Conf. Rob. Aut., 2006, pp. 1730–1736.

[84] T. Vose, P. Umbanhowar, K. Lynch, Friction-induced velocity fields for point parts sliding on a rigid oscillated plate, The International Journal of Robotics Research 28 (8) (2009) 1020–1039. doi:10.1177/0278364909340279.
URL http://ijr.sagepub.com/content/28/8/1020.abstract

[85] K. Sugawara, N. Correll, D. Reishus, Object transportation by granular convection using swarm robots, in: Distributed Algorithmic Robotics, 2012.

[86] E. D. Demaine, R. A. Hearn, Games of No Chance 3, Vol. 56, Mathematical Sciences Research Institute Publications, Cambridge University Press, 2009, Ch. Playing Games with Algorithms: Algorithmic Combinatorial Game Theory, pp. 3–56.
URL http://arXiv.org/abs/cs.CC/0106019

[87] A. T. Becker, Multi-robot position control with just 2 inputs: https://youtu.be/5p_xiad5-cw, YouTube (Apr 23 2013).
URL https://youtu.be/5p_XIad5-Cw

[88] A. T. Becker, G. Habibi, "Massive Uniform Manipulation: Control Large Populations of Simple Robots with a Common Input

Signal." http://www.mathworks.com/matlabcentral/fileexchange/42889, MATLAB Central File Exchange (Jul. 2013).
URL http://www.mathworks.com/matlabcentral/fileexchange/42889

[89] A. T. Becker, E. Demaine, S. Fekete, Controlling distributed particle swarms with only global signals, in: 3rd Workshop on Biological Distributed Algorithms (BDA), MIT, Cambridge, MA, USA, 2015.

[90] A. Becker, E. Demaine, S. Fekete, J. McLurkin, Particle computation: Designing worlds to control robot swarms with only global signals, in: IEEE International Conference on Robotics and Automation (ICRA), IEEE, Hong Kong, 2014, pp. 6751–6756. doi:10.1109/ICRA.2014.6907856.

[91] H. M. Shad, R. Morris-Wright, E. D. Demaine, S. P. Fekete, A. T. Becker, Particle computation: Device fan-out and binary memory, in: IEEE International Conference on Robotics and Automation (ICRA), Seattle, WA, USA, 2015.
URL https://github.com/aabecker/particleComputation/blob/master/fanout/FanOutgatesAndBinaryCounters.pdf

[92] A. Becker, E. Demaine, S. Fekete, G. Habibi, J. McLurkin, Reconfiguring massive particle swarms with limited, global control, in: International Symposium on Algorithms and Experiments for Sensor Systems, Wireless Networks and Distributed Robotics (ALGOSENSORS), Sophia Antipolis, France, 2013, pp. 51–66.

[93] A. T. Becker, E. Demaine, S. Fekete, H. Shad, R. Morris-Wright, Tilt: The video – designing worlds to control robot swarms with only global signals, in: 24th Multimedia Exposition in Computational Geometry (SoCG), Eindhoven, The Netherlands, 2015.

[94] S. Shahrokhi, A. T. Becker, "BlockPushingIROS2015", https://github.com/aabecker/swarmcontrolsandbox/blob/master/examplecontrollers/blockpushingiros20 (Jul. 2015).

[95] S. Shahrokhi, A. T. Becker, Stochastic swarm control, https://youtu.be/tcej-9e6-4o (Oct. 2015).
URL `https://youtu.be/tCej-9e6-4o`

[96] S. Shahrokhi, A. T. Becker, Stochastic swarm control with global inputs,, in: IEEE/RSJ International Conference on Intelligent Robots and Systems (IROS), 2015.